

**AN ASSESSMENT OF A FRACTIONAL-ORDER EPIDEMIOLOGICAL
SIMULATION AND THE INFLUENCE OF VACCINATION ON COVID-19
DYNAMICS IN BANGLADESH**

Most. Halimatuj Sadia¹, Md. Mojammel Haque² and M. Osman Gani³

¹Department of Mathematics and Statistics, Bangladesh University of Business and
Technology, Dhaka-1216, Bangladesh

E-mail: halimatuj@bubt.edu.bd

²Department of Mathematics, Dhaka University of Engineering and Technology, Gazipur-
1707, Bangladesh.

E-mail: mojammel@duet.ac.bd

³Department of Mathematics, Jahangirnagar University, Savar, Dhaka-1342, Bangladesh.

E-mail: osmangani2@juniv.edu

Abstract

This paper advises employing a fractional-value SEIR epidemic model with immunization for investigating at how COVID-19 spreads. It is clear that the model's solutions are positive and limited. When the fundamental reproduction number R_0 is less than 1, stability analysis shows that the equilibrium free of disease E_0 is asymptotically constant both locally and globally. When R_0 is more than 1, the equilibrium with infection E_1 is stable. Adding a vaccination parameter θ to the model considerably decreases the reproduction number R_0 . This shows how well vaccination works to stop the spread of disease. We use real-time COVID-19 data from Bangladesh to figure out the model parameters. We use the Adams-Bashforth-Moulton technique to run statistical simulations and show the results in figure. The findings indicate that the fractional-order SEIR model is superior and more effective in assessing the impacts of immunization compared to the conventional integer-order model.

Keywords: SEIR Model, Immunization, Stability analysis, Predictor–corrector method, Modelling analysis.

1. Introduction

Throughout history, humanity has faced numerous deadly epidemics and pandemics caused by viral infections, such as SARS, HIV/AIDS, H5N1, chickenpox, and smallpox. Research in life and matter sciences has focused on understanding and modeling the dynamics of such outbreaks [1] [2] [3] [4] [5]. Traditional compartmental models like SIS, SIR, and SIRS [6] [7] have been widely used to study disease transmission. However, these models often assume negligible incubation periods, which limits their applicability to diseases where latency plays a significant role. To address this, the SEIR model was introduced, incorporating an exposed (E) class to account for the incubation phase of infection.

Beyond incubation, other factors such as vaccination also critically influence the dynamics of infectious diseases. Vaccination plays a key role in reducing the spread of diseases, as it helps

establish herd immunity within populations. This protects individuals who are vaccinated and safeguards those who cannot be vaccinated due to medical reasons, thereby significantly altering the trajectory of infectious disease outbreaks. Gumel, McCluskey and Watmough [8] came up with an SEIR model in 2006 to look at the effects of an anti-SARS vaccine. They added a vaccinated (V) compartment to the model [9].

Nonetheless, the majority of these investigations relied on classical (integer-order) differential equations. Conversely, fractional-order differential models provide a more adaptable and precise methodology by integrating memory effects and genetic characteristics of biological processes. This study utilizes Caputo fractional-order derivatives to model the dynamics of a four-compartment SEIR system incorporating vaccination. This method facilitates a comprehensive comprehension of the temporal dissemination of diseases such as COVID-19 and the alleviating function of immunization [10].

Recently, the global scientific community has conducted substantial research to comprehend and manage the transmission of the highly contagious and lethal Coronavirus illness (COVID-19). Numerous mathematical models have been developed in epidemiology to clarify and predict the intricate processes that lead to infectious diseases. The foundational model was presented by Kermack and McKendrick in 1927. Subsequently, Tang et al. [11] presented a compartmental deterministic model that accounted for illness development, the epidemiological status of patients, and intervention techniques. The SIR model, extensively utilized in epidemiological research, acquired attention after its application by Anderson et al. in 1991 [12].

Anyway, these classical models are typically constructed with integer-order differential equations, which may insufficiently represent the memory and genetic effects present in several biological systems. Conversely, fractional-order differential equations have demonstrated efficacy in modelling the dynamics of numerous infectious diseases, providing enhanced flexibility and precision. Throughout the years, many techniques have been established for obtaining analytical and numerical solutions to these fractional-order models [13] [14] [15] [16].

Numerous fractional differential operators—including Caputo–Fabrizio, Riemann–Liouville, Caputo, Hadamard, Atangana–Baleanu, and Katugampola—have been utilized to analyze the dynamics of epidemic systems. This study employed the Caputo derivative, recognized for its nonlocal and nonsingular exponential kernel, to explore the dynamics of COVID-19 transmission. [17] [18] [19] [20] [21] [22] [23].

Recent studies have illustrated the relevance of fractional-order models across several epidemic scenarios, including the dynamic and computational analysis of a heroin epidemic model by Raza et al. [41], among others [24] [25] [26] [27] [28]. As previously said, vaccination is an essential instrument in combating infectious diseases. Vaccination has proven to be one of the most effective strategies to mitigate the spread of COVID-19. Theoretical analyses indicate that the COVID-19 vaccination method could attain disease eradication at lower vaccine coverage levels than conventional models. India commenced its COVID-19 vaccine initiative on January 16, 2021, and by May 10, 2021, more than 170 million doses had been delivered.

The campaign initially utilized Covishield protection, a domestically produced variant of the Oxford–AstraZeneca vaccine by the Serum Institute of India, and Covaxin, developed by Bharat Biotech. In April 2021, Sputnik V received approval as a third vaccination, with delivery commencing in late May 2021.

The following are the main goals of this work:

1. To examine the stability and dynamical behavior of a fractional-order SEIR model that includes vaccination.
2. To calculate the system's endemic and disease-free equilibrium points and the basic reproduction number R_0 .
3. To validate the analytical results and evaluate how well vaccinations work to stop the spread of COVID-19, numerical simulations will be run.

2. Formulation of the Model

The entire population $N(t)$ is separated into four epidemiological compartments at any given period $t \geq 0$:

$S(t)$ stands for susceptible individuals,

$E(t)$ for exposed persons (infected but not yet contagious),

$I(t)$ for infectious individuals, and

$R(t)$ for recovered individuals.

Thus, the total population is given by:

$$N(t) = S(t) + E(t) + I(t) + R(t)$$

The classical SEIR model with integer-order derivatives and vaccination is formulated as follows

$$\frac{dS}{dt} = \Lambda - \beta S(t)I(t) - \delta S(t) - \theta S(t)$$

$$\frac{dE}{dt} = \beta S(t)I(t) - (\delta + \rho)E(t)$$

$$\frac{dI}{dt} = \rho E(t) - (\delta + \sigma)I(t)$$

$$\frac{dR}{dt} = \sigma I(t) - \delta R(t) + \theta S(t)$$

With initial conditions $S(0) = S_0, E(0) = E_0, I(0) = I_0, R(0) = R_0$

Where,

- Λ : recruitment (birth) rate into the susceptible class,
- β : effective transmission rate,
- δ : natural death rate,
- θ : the rate of vaccination for people who are susceptible

- ρ : the rate at which people who are exposed become infectious,
- σ : recovery rate of infected individuals.

This integer-order SEIR model captures the essential disease dynamics and incorporates the effect of vaccination. In subsequent sections, we extend this framework to include fractional-order derivatives to better model the memory-dependent characteristics of real epidemics such as COVID-19.

3. Riemann–Liouville Fractional Integral

Let $f(t)$ be a function that is defined on the interval $[0, T]$ and let α be a number greater than 0. This is how you define the Riemann–Liouville fractional integral of order α of $f(t)$:

$$I^\alpha f(t) = \frac{1}{\Gamma(\alpha)} \int_0^t (t - y)^{\alpha-1} \cdot f(y) \cdot dy$$

where $\Gamma(\cdot)$ is the Gamma function.

3.1 Caputo Fractional Derivative

For a function $f(t)$, where $n \in \mathbb{N}$, the Caputo fractional derivative of order $\alpha \in (n-1, n)$ is defined as follows:

$$C_{D_t^\alpha} = \frac{1}{\Gamma(n-\alpha)} \int_0^t \frac{f^{(n)}(y)}{(t - y)^{\alpha-n+1}} \cdot dy$$

where $f^{(n)}(y)$ is the n -th derivative of $f(y)$, and $\Gamma(\cdot)$ is the Gamma function.

Following the Caputo approach, we improve the conventional integer-order model (1) by developing a fractional-order variant. The **system (1)** is represented by

$$\left. \begin{aligned} c_{D_t^\alpha} S(t) &= \Lambda - \beta S(t)I(t) - \delta S(t) - \theta S(t) \\ c_{D_t^\alpha} E(t) &= \beta S(t)I(t) - (\delta + \rho)E(t) \\ c_{D_t^\alpha} I(t) &= \rho E(t) - (\delta + \sigma)I(t) \\ c_{D_t^\alpha} R(t) &= \sigma I(t) - \delta R(t) + \theta S(t) \end{aligned} \right\} \dots\dots\dots (1)$$

With initial conditions $S(0) = S_0, E(0) = E_0, I(0) = I_0, R(0) = R_0$

3.2 Non-negativity and boundedness of Solutions

Proposition: The region $\Omega = \{(S, E, I, R) \in \mathbb{R}^4 : 0 < N \leq \frac{\Lambda}{\delta}\}$ is a positively invariant and non-negative region for the model for all $t \geq 0$.

Proof: we have,

$$\begin{aligned} C_{D_t^\alpha} (S+E+I+R) &= \Lambda - \delta(S+E+I+R) \\ C_{D_t^\alpha} N(t) &= \Lambda - \delta N(t) \end{aligned}$$

$$C_{D_t^\alpha N(t)+\delta N(t)=\Lambda}$$

Applying the Laplace conversion function $\mathcal{L}\{\cdot\}$ and the standard Laplace rule for a Caputo fractional derivative of order $0 < \alpha < 10$

$$\mathcal{L}\{C_{D_t^\alpha N(t)}\}(s) = s^\alpha f(s) - s^{\alpha-1}f(0+)$$

the linear fractional differential equation

$$C_{D_t^\alpha N(t)+\delta N(t)=\Lambda}$$

with initial value $N(0+) = N_0$ transforms as follows:

$$s^\alpha \tilde{N}(s) - s^{\alpha-1}N_0 + \delta \tilde{N}(s) = \frac{\Lambda}{s}$$

$$\tilde{N}(s) = \frac{\frac{\Lambda}{s} + s^{\alpha-1}N_0}{(s^\alpha + \delta)}$$

Where , $\tilde{N}(s) = \mathcal{L}\{N(t)(s)$

Using the reverse process Laplace conversion, we obtain

$$N(t) = N(0)E_{\alpha,1}(-\mu t^\alpha) + \Lambda t^\alpha E_{\alpha,\alpha+1}(-\Lambda t^\alpha)$$

Hence
$$N(t) = \left(N_0 - \frac{\Lambda}{\delta_0}\right)E_{\alpha,1}(-\mu t^\alpha) + \frac{\Lambda}{\delta}.$$

Thus,
$$\lim_{t \rightarrow 0} \text{Sup } N(t) \leq \frac{\Lambda}{\delta}$$

Therefore, the parameters S, E, I and R are all non-negative.

4. Fundamental Reproduction Number

The fundamental reproduction number R_0 is defined as the spectral radius (dominant eigenvalue) of the next-generation matrix FV^{-1} , Where, F denotes the array of new infection words, whereas V signifies the array of variations between compartments, encompassing recovery and mortality.

Mathematically,
$$R_0 = \rho(FV^{-1})$$

where $\rho(\cdot)$ represents the spectral radius, defined as the maximum absolute value of the eigenvalues.

Here, $F = \begin{bmatrix} 0 & \beta \frac{\Lambda}{\delta+\theta} \\ 0 & 0 \end{bmatrix}$ and $V = \begin{bmatrix} \delta + \rho & 0 \\ -\rho & \delta + \sigma \end{bmatrix}$

Therefore, the reproduction number $R_0 = \frac{\rho\beta\sigma}{(\delta+\theta)(\delta+\rho)(\delta+\sigma)}$

4.1 Stability Analysis

Determining the system's equilibrium is attainable by solving system (1). We could determine the healthy equilibrium points E_0 and the disease-causing equilibrium point E_1 of the system (1) by

$$C_{D_t^\alpha S(t)} = C_{D_t^\alpha E(t)} = C_{D_t^\alpha I(t)} = C_{D_t^\alpha R(t)} = 0$$

The model has two equilibrium points namely, $E_0 = (\frac{\Lambda}{\delta+\theta}, 0, 0, \frac{\Lambda\theta}{\delta(\delta+\theta)})$ and $E_1 = (S^*, E^*, I^*, R^*)$, Where, $S^* = \frac{(\delta+\rho)(\delta+\sigma)}{\beta\rho}$, $E^* = \frac{(\delta+\sigma)}{\rho} I^*$, $I^* = \frac{\Lambda\rho}{(\delta+\rho)(\delta+\sigma)} - \frac{(\delta+\theta)}{\beta}$, $R^* = \frac{\sigma I^* + \theta S^*}{\delta}$.

The Jacobian matrix (J) of the simulation model (1) at the point (S, E, I, R) is expressed as

$$J = \begin{bmatrix} -\beta I - \delta - \theta & 0 & -\beta S & 0 \\ \beta I & -(\delta + \rho) & \beta S & 0 \\ 0 & \rho & -(\delta + \sigma) & 0 \\ 0 & 0 & \sigma & -\delta \end{bmatrix}$$

Theorem 1: The healthy equilibrium point E_0 of system (1) is locally asymptotically steady when R_0 is lower than 1, and becomes unstable when R_0 crosses 1.

Proof: the Jacobian matrix J at E_0 becomes

$$J(E_0) = \begin{bmatrix} -\delta - \theta & 0 & -\beta \frac{\Lambda}{\delta+\theta} & 0 \\ \beta I & -(\delta + \rho) & \beta \frac{\Lambda}{\delta+\theta} & 0 \\ 0 & \rho & -(\delta + \sigma) & 0 \\ 0 & 0 & \sigma & -\delta \end{bmatrix}$$

The solutions to the characterized equation are presented as $(-\delta - \theta)$, $-\delta$, $-(\delta + \sigma)$ and $(\delta + \rho) (R_0 - 1)$. Depending on whether $R_0 < 1$ or $R_0 > 1$, the equilibrium point E_0 is either locally asymptotically steady or unsteady.

Theorem 2: When $R_0 > 1$, the infection-endemic equilibrium point E_1 of system (1) is locally asymptotically steady. When $R_0 < 1$, it becomes unstable.

Proof: The Jacobian matrix J at E_1 becomes

$$J = \begin{bmatrix} -\beta I^* - \delta - \theta & 0 & -\beta S^* & 0 \\ \beta I^* & -(\delta + \rho) & \beta S^* & 0 \\ 0 & \rho & -(\delta + \sigma) & 0 \\ 0 & 0 & \sigma & -\delta \end{bmatrix}$$

Where,
$$p = \beta I^* + 3\delta + \rho + \sigma + \theta$$

$$q = (\beta I^* + \delta + \theta)(2\delta + \rho + \sigma) + (\delta + \rho)(\delta + \sigma) - \beta\rho S^*$$

$$r = (\beta I^* + \delta)((\delta + \rho)(\delta + \sigma) - (\delta + \theta)\beta\rho S^*)$$

Using Routh-Hurwitz criteria, the model (1) is asymptotically steady in locally at E_1 as $p > 0$, $q > 0$, $pq > 0$.

5. Application of the Predictor-Corrector Method to the SEIR Model

For situations involving fractional order initial values, the Aadmms-Bashforth-Moultron approach is the numerical method that has been applied the most typically. The Adams-Bashforth-Moulton approach offers a robust framework for addressing the complexities associated with fractional-order dynamics in epidemiological models. By effectively incorporating past information and adjusting predictions accordingly, this method enhances the accuracy of the SEIR model's forecasting capabilities in various scenarios.

Let us consider

$${}^C D_t^\alpha L_j(t) = g_j(t, L_j(t)), \quad L_j(0) = L_{j0}^r$$

$$r = 0, 1, 2, \dots, [\alpha] j \in \mathbb{N}$$

Where, The Volterra integral equation is the same as $L_j^r \in \mathbb{R}$

$$L_j(t) = \sum_{n=0}^{[\alpha]-1} L \frac{t^n}{n!} + \frac{1}{\Gamma(\alpha)} \int_0^t (t-u)^{\alpha-1} g_j(u, L_j(u)) du, \quad j \in \mathbb{N}$$

Here is a description of the algorithm.

Let $T = h\hat{n}$, $t_n = nh$, $n = 0, 1, 2, \dots, \hat{n}$.

Corrector formulae:

$$S_{n+1} = S_0 + \frac{h^{\alpha_1}}{\Gamma(\alpha_1 + 2)} (\Lambda - \beta S_{n+1}^p I_{n+1}^p - \delta S_{n+1}^p - \theta S_{n+1}^p) +$$

$$\frac{h^{\alpha_1}}{\Gamma(\alpha_1 + 2)} \sum_{j=0}^n \alpha_{1,j,n+1} (\Lambda - \beta S_j I_j - \delta S_j - \theta S_j)$$

$$E_{n+1} = E_0 + \frac{h^{\alpha_2}}{\Gamma(\alpha_2 + 2)} (\beta S_{n+1}^p I_{n+1}^p - (\delta + \rho) E_{n+1}^p) +$$

$$\frac{h^{\alpha_2}}{\Gamma(\alpha_2 + 2)} \sum_{j=0}^n \alpha_{2,j,n+1} (\beta S_j I_j - (\delta + \rho) E_j)$$

$$I_{n+1} = I_0 + \frac{h^{\alpha_3}}{\Gamma(\alpha_3 + 2)} (\rho E_{n+1}^p - (\delta + \sigma) I_{n+1}^p) + \frac{h^{\alpha_3}}{\Gamma(\alpha_3 + 2)} \sum_{j=0}^n \alpha_{3,j,n+1} (\rho E_j - (\delta + \sigma) I_j)$$

$$R_{n+1} = R_0 + \frac{h^{\alpha_4}}{\Gamma(\alpha_4 + 2)} (\sigma I_{n+1}^p - \delta R_{n+1}^p + \theta S_{n+1}^p) + \frac{h^{\alpha_4}}{\Gamma(\alpha_4 + 2)} \sum_{j=0}^n \alpha_{4,j,n+1} (\sigma I_j - \delta R_j + \theta S_j)$$

Predictor formulae:

$$S_{n+1} = S_0 \frac{h^{\alpha_1}}{\Gamma(\alpha_1)} \sum_{j=0}^n \beta_{1,j,n+1} (\Lambda - \beta S_j I_j - \delta S_j - \theta S_j)$$

$$E_{n+1} = E_0 + \frac{h^{\alpha_2}}{\Gamma(\alpha_2)} \sum_{j=0}^n \beta_{2,j,n+1} (\beta S_j I_j - (\delta + \rho) E_j)$$

$$I_{n+1} = I_0 + \frac{h^{\alpha_3}}{\Gamma(\alpha_3)} \sum_{j=0}^n \beta_{3,j,n+1} (\rho E_j - (\delta + \sigma) I_j)$$

$$R_{n+1} = R_0 + \frac{h^{\alpha_4}}{\Gamma(\alpha_4)} \sum_{j=0}^n \beta_{4,j,n+1} (\sigma I_j - \delta R_j + \theta S_j)$$

Where,

$$\alpha_{i,j,n+1} = \begin{cases} n^{\alpha+1} - (n - \alpha)(n + 1)^\alpha, & \text{if } j = 0 \\ (n - j + 2)^{\alpha+1} + (n - j)^{\alpha+1} - 2(n - j + 1)^{\alpha+1}, & \text{if } 0 \leq j \leq n \\ 1, & \text{if } j = 1 \end{cases}$$

And

$$\beta_{i,j,n+1} = \frac{h^{\alpha_i}}{\alpha} [(n + 1 - j)^{\alpha_i} - (n - j)^{\alpha_i}], 0 \leq j \leq n \text{ and } i = 1,2,3,4.$$

5.1 Modelling generated from numerical data

In this section, we conduct comprehensive numerical simulations of the results generated by the Adams-Bashforth-Moulton predictor–corrector system using mathematical software. We examine both the vaccine-free scenario, represented by $\eta = 0$, and the scenario with vaccines, indicated by $\eta \neq 0$. The aim of these simulations is to clarify the dynamics of disease transmission under both conditions, emphasising the influence of vaccination on transmission rates and the overall immunity of the population.

The following are approximate values of the parameters for COVID-19 in Bangladesh:

Parameter	Value [non-vaccinated]	Value [vaccinated]	Reference
Λ	50	50	Estimated
β	0.0002	0.0002	Estimated
δ	0.0053	0.0053	Estimated
θ	0.0	0.03	Model to fit
ρ	0.019	0.019	[59, 60]
σ	0.0186	0.0186	[59, 60]

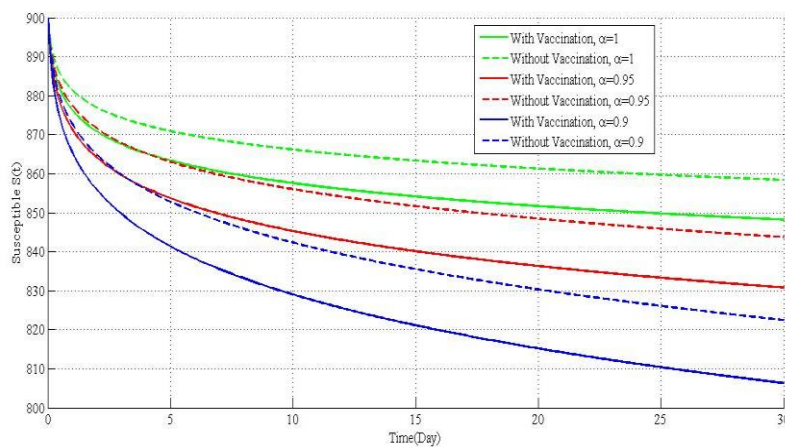


Fig 1: Graph of $S(t)$ for varying values of α in relation to time (days) with and without vaccine

Figure 1 shows how the number of people who are susceptible changes over time for different values of the fractional value α , in both cases: with and without vaccination. The number of people that are sensitive goes down with time for all values of α . But at any given time, there are more people who are likely to get sick when α is smaller. This shows that fractional-order derivatives provide a memory effect that changes the pace of deterioration. This memory effect highlights the nuanced dynamics of disease transmission and the impact of vaccination strategies. As a result, understanding these fractional-order models can enhance public health responses by allowing for more tailored interventions that consider the varying susceptibility of populations over time. This suggests that incorporating fractional dynamics provides a more nuanced understanding of susceptibility over time. Additionally, the plots confirm that vaccination consistently reduces the number of susceptible individuals compared to the non-vaccination case for all values of α , as expected.

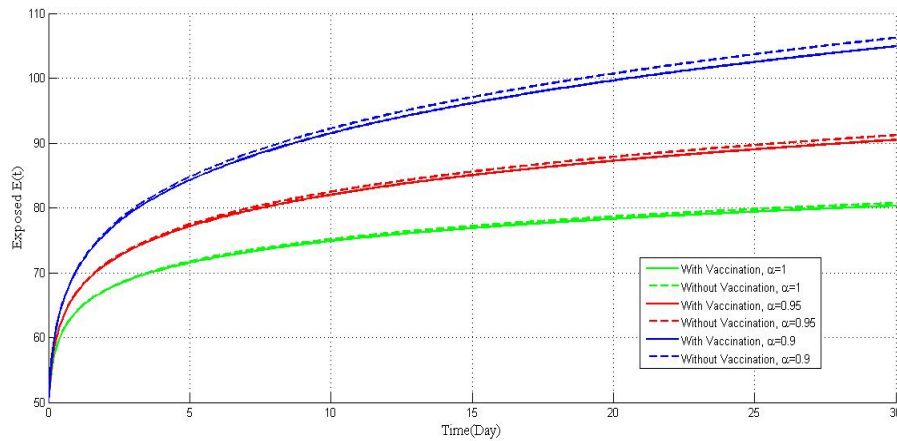


Fig. 2: Graph of $E(t)$ for varying values of α in relation to time (days) with and without vaccine

Figure 2 illustrates the temporal progression of the exposed population for different values of the fractional number α , accounting for both vaccinated and unvaccinated situations. For all values of α , the population of exposed individuals escalates over time. At each given time t , the quantity of exposed people escalates as the fractional order α diminishes. This graph illustrates the influence of memory effects intrinsic to fractional-order models, which often decelerate the rate of exposure advancement. Moreover, the incorporation of vaccination yields a consistently reduced number of exposed individuals relative to the non-vaccination scenario across all values of α , which is consistent with anticipated epidemiological results. This observation highlights the critical role of vaccination in controlling the spread of infectious diseases, reinforcing the importance of public health initiatives. Consequently, it becomes evident that targeted vaccination strategies can significantly alter the trajectory of disease transmission, underscoring the need for ongoing research in this area.

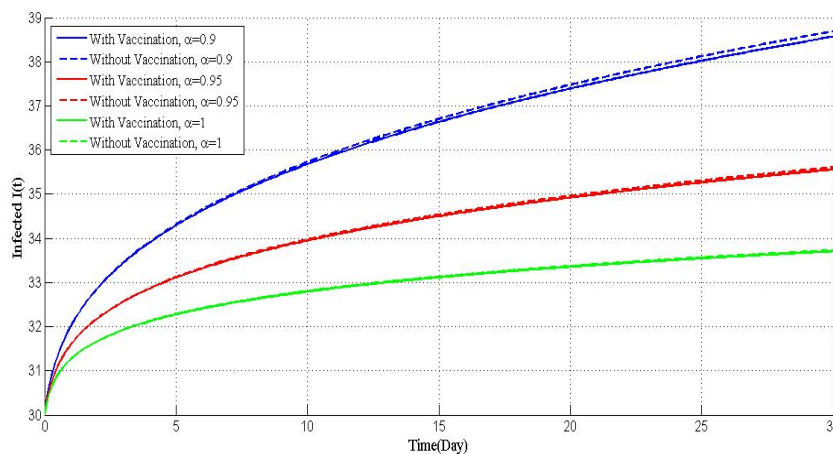


Fig. 3: Graph of $I(t)$ for varying values of α in relation to time (days) with and without vaccine

Figure 3 depicts the temporal dynamics of the infected population across different fractional order values α , accounting for both vaccinated and unvaccinated conditions. For all fractional

orders, the population of infected people diminishes significantly over time. Furthermore, the incorporation of vaccination significantly hastens this reduction, leading to a persistently decreased incidence of illnesses relative to the non-vaccination scenario. This evidence illustrates the synergistic effect of fractional-order dynamics and vaccination in reducing disease spread. This reduction in disease spread highlights the importance of implementing vaccination strategies along with fractional-order modelling approaches in public health planning. By understanding these dynamics, health authorities can better tailor interventions to mitigate the impact of infectious diseases on populations.

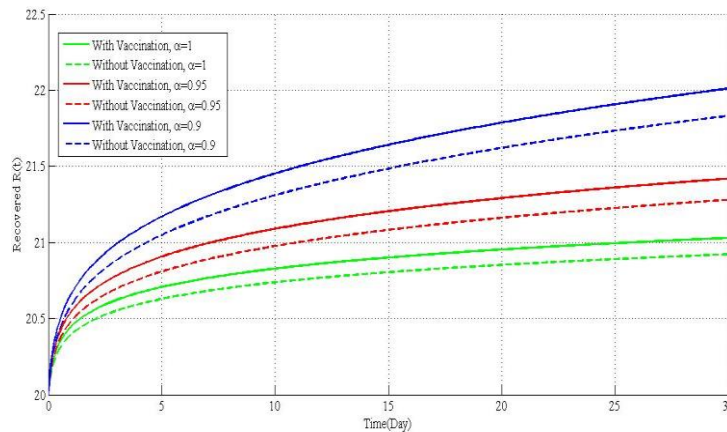


Fig. 4: Graph of $R(t)$ for varying values of α in relation to time (days) with and without vaccine

Figure 4 illustrates the temporal progression of the recovered population for different values of the fractional order α . The graph unequivocally demonstrates that the quantity of recovered individuals escalates over time for all examined values of α . Moreover, the findings indicate that vaccination substantially influences this increase since the count of recovered individuals is greater when vaccination is present. This result underscores the beneficial impact of immunization in expediting healing among the populace. Additionally, it highlights the importance of implementing vaccination strategies as a critical component in public health efforts. By fostering higher recovery rates, we can significantly mitigate the impact of diseases and protect the overall health of the community.

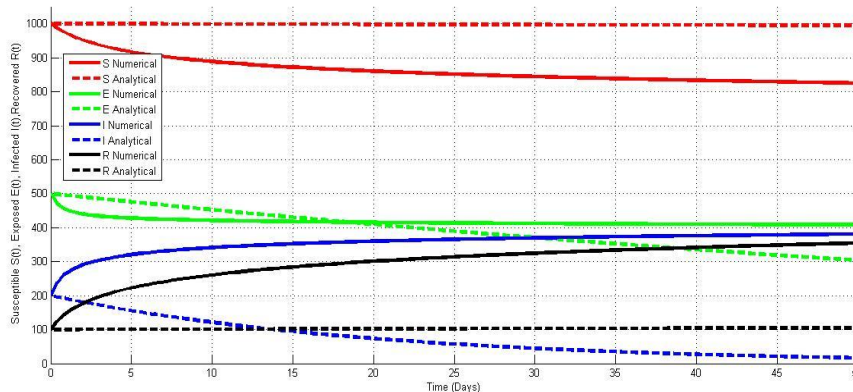


Fig.5: Graph of SEIR model over time using analytical and numerical method

Figure 5 illustrates the time series analysis of the SEIR model with vaccination at $R_0 = 0.0053$, utilizing the parameter values specified in Table 1. The two equilibrium points are $E_0 = (1428.57, 0, 0, 8571.44)$ and $E_1 = (538.125, 0.525, 289.57, 902.015)$. The results indicate that the model system (2.5) possesses an endemic equilibrium and is asymptotically unsteady with differing initial values, corroborating our theoretical findings in **Theorem 2**. This instability suggests that small perturbations in the initial conditions can lead to significant deviations from the predicted outcomes, emphasizing the importance of accurate parameter estimation in the SEIR model for vaccination. Furthermore, the presence of the endemic equilibrium highlights the necessity for ongoing vaccination efforts to manage disease prevalence effectively.

Effect of β on the fundamental reproduction number

Value of β	Value of R_0
0.001	0.0372
0.02	0.7433
0.3	11.1498
0.5	18.5830
0.87	32.3345

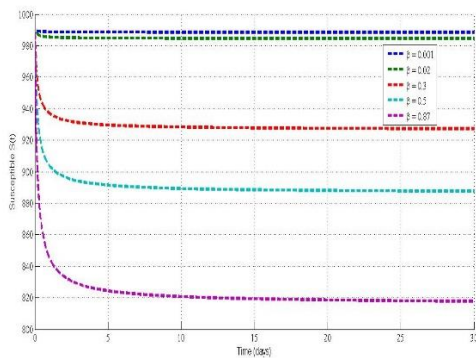


Fig.6(a) Impact of β on susceptible class.

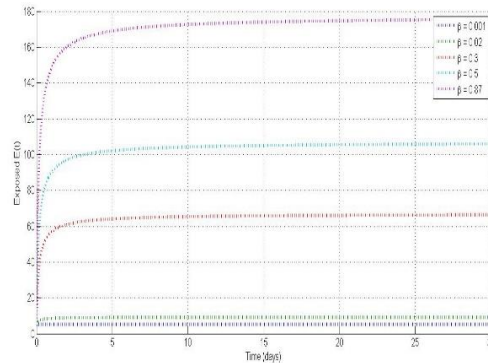


Fig.6(b) Impact of β on exposed class

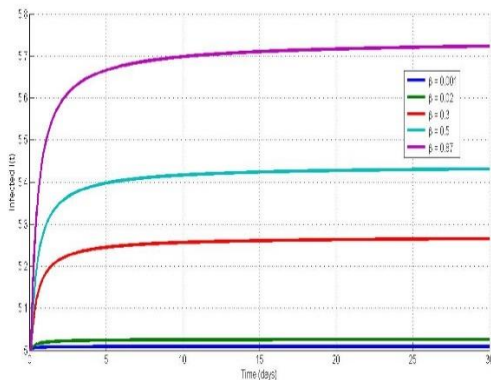


Fig.6(c) Impact of β on infected class.

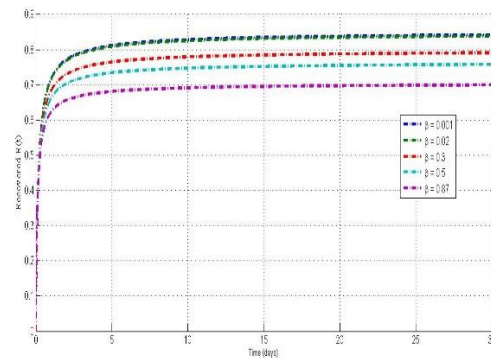


Fig.6(d) Impact of β on recovered class.

Figure 6 depicts the temporal dynamics of the SEIR model compartments susceptible (S), Exposed (E), Infected (I), and Recovered (R) for varying transmission rates inside a fractional-order derivative framework of order. The model integrates the influences of natural mortality rate, vaccination and illness advancement. In the Susceptible compartment (S), an increase in β results in a more rapid decrease in the population of susceptible individuals. This is anticipated, as an elevated transmission rate results in a greater number of individuals being exposed more rapidly due to more interactions with sick individuals. The Exposed compartment (E) indicates that an increase leads to a more pronounced initial surge in exposed people, signifying accelerated disease transmission. The rate at which exposed individuals transition to the infected category also affects the peak and decline of $E(t)$. An increase in β substantially influences both the peak height and timing of the infected compartment (I). Increased values result in a quicker and elevated peak, indicating swift transmission, whereas diminished values prolong and diminish the outbreak magnitude, demonstrating a more regulated illness development. In the Recovered compartment (R), recovery is contingent upon the infected class; hence, an increased β results in a higher number of infections and, subsequently, more recoveries. $R(t)$ escalates more rapidly and attains a superior ultimate level with greater β .

The image illustrates that the transmission rate is a pivotal element in regulating illness dissemination. Mitigating β (e.g., via measures like masks, social separation, and public awareness) decelerates the pandemic, safeguarding the susceptible population and flattening the infection curve. This approach not only helps to protect those at higher risk but also provides healthcare systems with the necessary time to manage resources effectively. By implementing this strategy, communities can work together to minimise the overall impact of the virus and promote public health.

6. Conclusion

This work examined the SEIR epidemic model, utilizing fractional-order derivatives via the Caputo operator for orders $0 < \alpha \leq 10$ and integrating a vaccination component. Using COVID-19 case data from India until August 1, 2021, we calculated the basic reproduction number R_0 as 3.67 in the absence of immunization and 0.55 with vaccination. This finding unequivocally illustrates that the incorporation of the vaccination parameter θ markedly diminishes the reproductive capacity of the virus. The parameter values used in equation (2.8) were obtained from real-time data sources [59, 60] and are shown in Table 1. Fractional-order derivatives are advantageous for modelling intricate real-world events because of their adaptability and decreased inaccuracy, particularly when used with imprecise real-time data and surpassing conventional integer-order models in certain contexts. Our data confirm that immunization is essential for controlling and preventing the transmission of COVID-19. We may expand the suggested model to analyses the dynamics of other infectious illnesses and assess the effectiveness of vaccination in mitigating their spread. Our data suggests that healthcare authorities, decision-makers, and policy experts should priorities the deployment of effective vaccination measures to address viral epidemics. Preemptive measures are essential for reducing extensive transmission and mitigating population effects.

Measures including lockdowns, curfews, limited mobility zones, and checkpoints can effectively curb the spread. The current study aims to comprehend how decreases in interpersonal interaction affect the dynamics of disease transmission. Our future target is to enhance the SEIR framework by integrating diverse levels of population isolation and interaction. This enhancement will allow for a more nuanced understanding of how varying degrees of isolation affect infection rates, ultimately providing valuable insights for policymakers. By simulating different scenarios of interaction and isolation, we aim to identify the most effective strategies for controlling future outbreaks.

Acknowledgement: I would like to thank my supervisor **Prof. Dr. Mohammad Osman Gani** for supporting the entire work.

Conflicts of Interest

The authors declare no conflicts of interest regarding the publication of this paper.

Funding

self-funding.

References

- [1] S. M. A. M. S. R. B. Paul, " Dynamics of SIQR epidemic model with fractional order derivative. Partial Differ. Equ.," *Applied math* , 2022.
- [2] " Pongkitivanichkul, C., Samart, D., Tangphati, T., Koomhin, P., Pimton, P., Dam-o, P., Payaka, A., Chan- nuie, P.: Estimating the size of COVID-19 epidemic outbreak. Phys. Scr. 95, 085206 (2020)".
- [3] "Liu, X.X., Hu, S., Fong, S.J., Crespo, R.G., Viedma, E.H.: Modelling dynamics of coronavirus disease 2019 spread for pandemic forecasting based on Simulink. Phys. Biol. 18(4), 045003 (2021)".
- [4] "Pongsumpun, P., Tang, I.M.: Dynamics of a new strain of the H1N1 influenza a virus incorporating the effects of repetitive contacts. Comput. Math. Methods Med. 2014, 487974 (2014). <https://doi.org/10.1155/2014/487974>".
- [5] " Upadhyay, R.K., Kumari, N., Rao, V.S.H.: Modeling the spread of bird flu and predicting outbreak diversity. Nonlinear Anal. Real World Appl. 9, 1638–1648 (2008)".
- [6] " Blackwood, J.C., Childs, L.M.: An introduction to compartmental modeling for the budding infectious disease modeler. Lett. Biomath. 5(1), 195–221 (2018)".
- [7] " Shereen, M.A., Khan, S.: COVID-19 infection: origin, transmission, and characteristics of human coro- naviruses. J. Adv. Res. 24, 91–98 (2020)".
- [8] "Gumel, A.B., McCluskey, C., Watmough, J.: An SVEIR model for assessing potential impact of an imperfect anti-SARS vaccine. Math. Biosci. Eng. 3(3), 485–512 (2006)".

- [9] " Yuan, C., Jiang, D., Regan, D.O., Agarwal, R.P.: Stochastically asymptotically stability of the multi- group SEIR and SIR models with random perturbation. *Commun. Nonlinear Sci. Numer. Simul.* 17(6), 2501–2516 (2012)".
- [10] " Zhu, L.H., Wang, X.W., Zhang, H.H., Shen, S.L., Li, Y.M., Zhou, Y.D.: Dynamics analysis and optimal control strategy for a SIRS epidemic model with two discrete time delays. *Phys. Scr.* 95, 035213 (2020)".
- [11] " Yuan, C., Jiang, D., Regan, D.O., Agarwal, R.P.: Stochastically asymptotically stability of the multi- group SEIR and SIR models with random perturbation. *Commun. Nonlinear Sci. Numer. Simul.* 17(6), 2501–2516 (2012)".
- [12] " Ghanbari, B., Kumar, S., Kumar, R.: A study of behaviour for immune and tumor cells in immune genetic tumour model with non-singular fractional derivative. *Chaos Solitons Fractals* 133, 109619 (2020)".
- [13] " Kumar, S., Kumar, A., Baleanu, D.: Two analytical methods for time-fractional nonlinear coupled Boussi- nesq–Burger’s equations arise in propagation of shallow water waves. *Nonlinear Dyn.* 85, 699–715 (2016)".
- [14] " Shaikh, A., Sontakke, B.R.: Impulsive initial value problems for a class of implicit fractional differential equations. *Comput. Methods Differ. Equ.* 8(1), 141–154 (2020)".
- [15] " Daftardar-Gejji, V., Jafari, H.: An iterative method for solving nonlinear functional equations. *J. Math. Anal. Appl.* 316, 753–763 (2006)".
- [16] " Sontakke, B.R., Shaikh, A.S., Nisar, K.S.: Approximate solutions of a generalized Hirota-Satsuma coupled KdV and a coupled mKdV systems with time fractional derivatives. *Malays. J. Math. Sci.* 12(2), 173–193 (2018)".
- [17] " Atangana, A.: Modelling the spread of COVID-19 with new fractal-fractional operators: can the lockdown save mankind before vaccination? *Chaos Solit. Fractals.* 136, 109860 (2020)".
- [18] " Akdim, K., Ez-Zetouni, A., Zahid, M.: The influence of awareness campaigns on the spread of an infectious disease: a qualitative analysis of a fractional epidemic model. *Model. Earth Syst. Environ.* (2021). [https:// doi.org/10.1007/s40808-021-01158-9](https://doi.org/10.1007/s40808-021-01158-9).
- [19] " Akdim, K., Ez-Zetouni, A., Zahid, M.: The influence of awareness campaigns on the spread of an infectious disease: a qualitative analysis of a fractional epidemic model. *Model. Earth Syst. Environ.* (2021). [https:// doi.org/10.1007/s40808-021-01158-9](https://doi.org/10.1007/s40808-021-01158-9).
- [20] " Shaikh, A., Tassaddiq, A., Nisar, K.S., Baleanu, D.: Analysis of differential equations involving Caputo- Fabrizio fractional operator and its applications to reaction–diffusion equations. *Adv. Differ. Equ.* 178, 1–14 (2019)".
- [21] " Kumar, S.: A new analytical modelling for fractional telegraph equation via Laplace transform. *Appl. Math. Model.* 38, 3154–3163 (2014)".

- [22] " Kumar, S.: A new analytical modelling for fractional telegraph equation via Laplace transform. *Appl. Math. Model.* 38, 3154–3163 (2014)".
- [23] " Atangana, A.: Modelling the spread of COVID-19 with new fractal-fractional operators: can the lockdown save mankind before vaccination? *Chaos Solit. Fractals.* 136, 109860 (2020)".
- [24] " Ahmed, N., Raza, A., Rafiq, M., Ahmadian, A., Batool, N., Salahshour, S.: Numerical and bifurcation analysis of SIQR model. *Chaos Solitons Fractals* 150, 111133 (2021)".
- [25] " Raza, A., Chu, Y.M., Bajuri, M.Y., Ahmadian, A., Ahmed, N., Rafiq, M., Salahshour, S.: Dynamical and nonstandard computational analysis of heroin epidemic model. *Res. Phys.* 34, 105245 (2022)".
- [26] " Haidong, Q., Arfan, M., Salimi, M., Salahshour, S., & Ahmadian, A. (2021). Fractal–fractional dynamical system of Typhoid disease including protection from infection. *Eng. Comput.*, 1–10."
- [27] " Salahshour, S., Ahmadian, A., Abbasbandy, S., Baleanu, D.: M-fractional derivative under interval uncertainty: theory, properties and applications. *Chaos Solit. Fractals.* 117, 84–93 (2018)".
- [28] " Ahmad, S.W., Sarwar, M., Shah, K., Ahmadian, A., Salahshour, S.: Fractional order mathematical modeling of novel corona virus (COVID-19). *Math. Meth. Appl. Sci.* 1–14 (2021)".